https://doi.org/10.20965/ijat.2018.p0004

Review:

MEMS Sensor Devices with a Piezo-Resistive Cantilever

Kiyoshi Matsumoto[*,†] **and Isao Shimoyama**[**]

[*]Department of Mechanical Engineering, Faculty of Science and Engineering, Toyo University
2100 Kujirai, Kawagoe, Saitama 350-8585, Japan
[†]Corresponding author, E-mail: matsumoto064@toyo.jp
[**]Department of Mechano-Informatics, Graduate School of Information Science and Technology, The University of Tokyo, Tokyo, Japan

[Received June 28, 2017; accepted October 6, 2017]

We have engaged in researching and developing a large number of sensor devices using piezo-resistive cantilevers. The important technical features of our sensor devices lie in their very high detection sensitivity that has been achieved by the use of cantilevers of a very thin structure: as a typical example, force-detection sensitivity of about 10 pN has been achieved by using cantilevers of 300-nm thickness. This paper presents our developed sensor devices and applications and their respective features: more specifically, devices to directly measure object-contacting forces, devices embedded in an elastic body to measure its deformations, devices to measure air flows and vibrations, devices to measure differential air pressure, devices to measure differential pressure between cavities and external environment, and devices with cantilevers arranged on the liquid interface.

Keywords: cantilever, sensor, piezo-resistive, MEMS

1. Introduction

This paper describes micro-electro-mechanical-systems (MEMS) based sensor devices and applications employing piezo-resistive cantilevers. A cantilever refers to a cantilevered beam, and this paper deals with micro-cantilevers with sizes of several hundred microns or less. By creating a piezo-resistive part at the micro-cantilever's base, where resistance changes during deformation, the micro-cantilever's inclinations can be detected as resistance changes.

A micro-cantilever was used as the probe of an atomic force microscope (AFM), a kind of scanning probe microscope (SPM), for the first time. The AFM can image not only electroconductive but also non-electroconductive specimens with very high definition in both the vertical and horizontal directions. In measuring resistance, the micro-cantilever's deformation needs to be detected with high resolution by scanning a specimen in contact or in close proximity. Such deformations used to be detected by several different methods, such as using tunneling current, optical interference, optical lever, and capacitance, which required large and complex apparatus. In contrast, Reference [1] proposed to combine the micro-cantilever and piezo-resistance effects to detect the micro-cantilever's deformations as resistance changes. Piezo-resistance effects, also known as piezoelectric effects, represent any changes in electric resistance or conductivity due to changes in the crystal lattice structure or in the electron energy band structure of metals or semiconductors, which are caused by pressure or distortions. It used to be employed in semiconductor strain gauges or in the detection mechanism of pressure sensors.

We have engaged in researching and developing a large number of sensor devices using piezo-resistive cantilevers. The important technological features of our design lie in using a very thin cantilever structure to achieve very high detection sensitivity. As a typical example, cantilevers as thick as 300 nm have achieved force resolutions of around 10 pN [2]. Using these piezo-resistive cantilevers, we have detected forces, pressures, and displacements with high sensitivity, and have developed devices to detect various physical quantities by applying such cantilevers. In this paper, we categorize by principle the sensor devices and applications we have so far researched and developed.

2. Structure of Piezo-Resistive Cantilevers and Fabrication Process

Figure 1 shows a typical example of a piezo-resistive cantilever: it is 300 nm thick and has two piezo-resistive hinged parts at its base so that its inclinations can be detected as resistance changes. It is 100 μm long and 100 μm wide, which may vary with applications.

Figure 2 shows the fabrication process of the piezo-resistive cantilever [2, 3]: the side view in each step corresponds to the A–A′ cross section of the bird's-eye view. The substrate material is a p-type-doped silicon-on-insulator (SOI) wafer. The SOI wafer for the device has a 290 nm-thick Si layer and a 400 nm-thick SiO_2 layer, and a 300 μm-thick Si layer for handling. In the first step, an n-type piezo-resistive layer is formed on the SOI wafer by rapid thermal diffusion: the piezo-resistive layer is 100 nm thick and the sheet has a resistance of 200 Ω/sq. In the next step, an Au layer is formed and patterned. With the Au layer as a mask, the device's Si layer is etched by inductively coupled plasma reactive ion etching (ICP-RIE). The Au layer is etched once more to remove the metal layer from the surface of the piezo-resistive part,

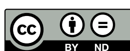

© Fuji Technology Press Ltd. Creative Commons CC BY-ND: This is an Open Access article distributed under the terms of the Creative Commons Attribution-NoDerivatives 4.0 International License (http://creativecommons.org/licenses/by-nd/4.0/).

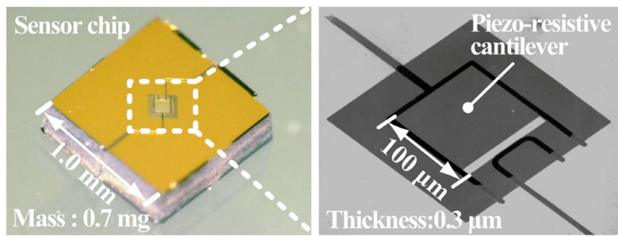

Fig. 1. Typical example of piezo-resistive cantilever.

(a) Thermal diffusion to dope N-dopant to an SOI wafer.

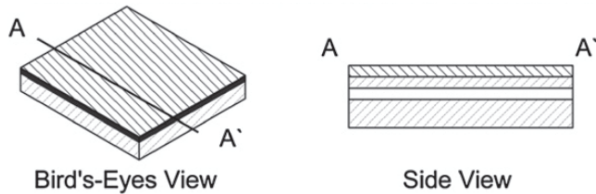

(b) Depositing Au layer, and patterming AU/Si layers.

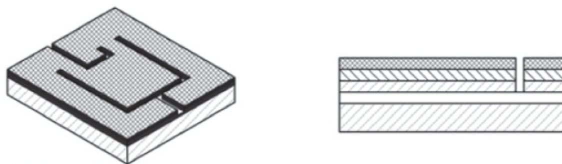

(c) Patternubg Au layer.

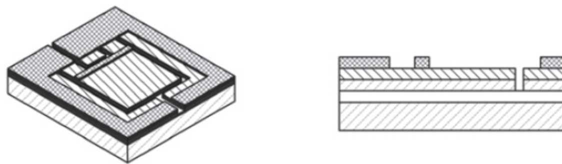

(d) Removing bottom SiO_2/Si layers.

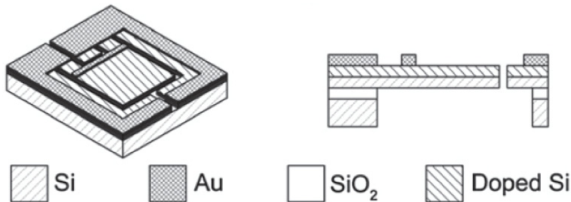

Source: [3]

Fig. 2. Production process of piezo-resistive cantilever [3].

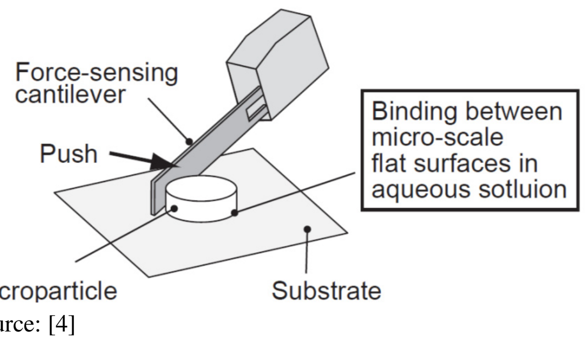

Source: [4]

Fig. 3. Measurements of sticking forces of microparticles [4].

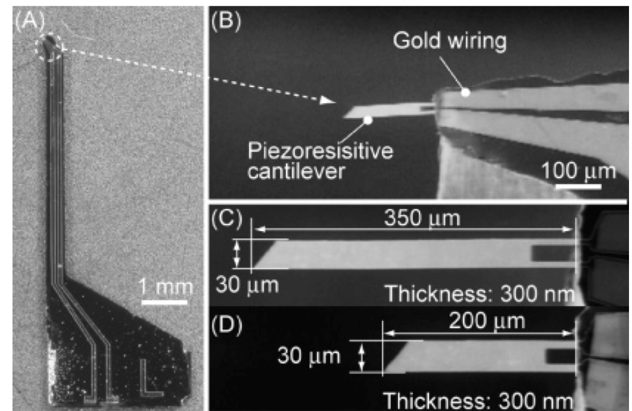

Source: [4]

Fig. 4. Piezo-resistive cantilevers to measure sticking forces [4].

and an electrode is formed. Then, the handling Si layer is etched by ICP-RIE and the cantilever is released by etching the SiO_2 layer in HF vapor.

3. Sensor Devices Using Piezo-Resistive Cantilevers

3.1. Devices to Directly Measure Object-Contacting Forces

The simplest application of piezo-resistive cantilevers is to measure the forces involved in handling an object with the cantilever's tip. Studies on applications of piezo-resistive cantilevers include: a study to measure sticking forces of microparticles to a wall in liquid [4]; a study to measure the optical near-fields in the neighborhood of a micro-aperture by scanning a fluorescent bead [5]; a study to detect protein by measuring the sticking force between the receptor-applied cantilever and ligands [6]; a study to measure sticking forces between the ligand-applied cantilever and the receptor on the cell surface [7]; and studies to measure the vibrations and pressure distributions of microdroplets [8–10].

Herein, we present a study to measure the sticking forces of microparticles to the wall surface [4]. The final goal of the study is to self-assemble microstructures by stirring microparticles in liquid. In order to achieve the study goal, we need to quantitatively evaluate the sticking forces of microparticles. **Fig. 3** shows how to measure sticking forces of microparticles, by laterally pushing the cantilever onto the particle sticking to the wall surface in liquid and measuring the forces when the particles slip away.

Figure 4 shows the prototyped force-sensing cantilever. In order to enhance its force-detection sensitivity, we have elongated the cantilever to 200 μm and 350 μm. The 350 μm-long cantilever is designed to have a spring stiffness of 1.0 nN/μm and a sensitivity of 220 $\mu\varepsilon/\mu$m to displacements, in which case its sensitivity to forces becomes 220 $\mu\varepsilon$/nN, and the experiments have demonstrated similar values.

Figure 5 shows the measurements of the sticking forces of microparticles. When the cantilever is laterally moved

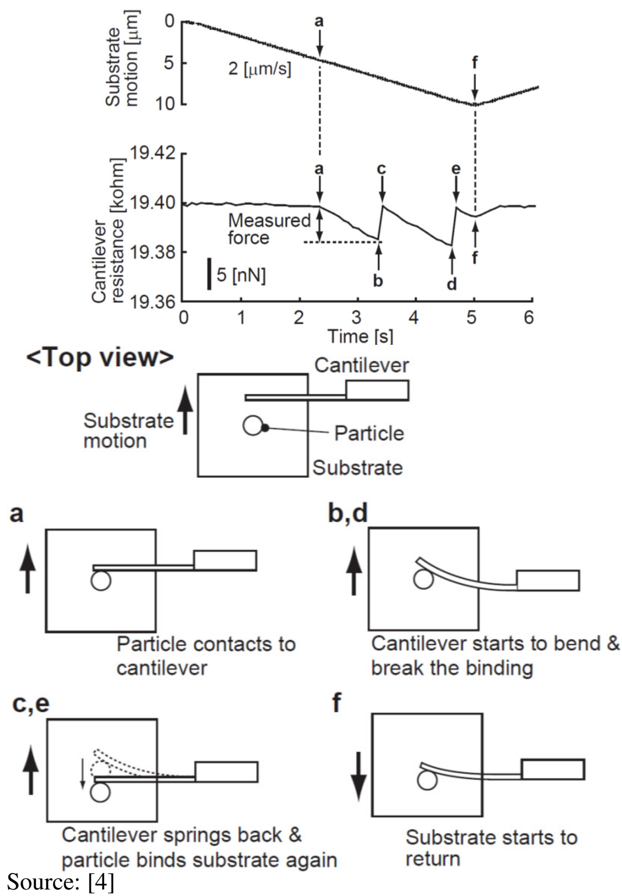

Source: [4]

Fig. 5. Example of measurement of binding forces [4].

closer to the particle at a constant rate, it contacts the particle at point a, increasing its pushing force. The particle detaches from the wall surface at point b, and the cantilever springs back to the original position. The particle again sticks to the wall surface at point c, and detaches again at point d. The experiments have enabled us not only to measure the sticking forces, but also to clearly observe how the particle sticks and slips away.

Now, we present a study on the measurements of binding forces between the ligand-applied cantilever and the receptor on the cell surface [7], which evaluates the density of the cell's epidermal growth factor receptor (EGFR) in terms of its sticking force to ligands. **Fig. 6** shows the experiments we have conducted. With the cantilever's tip applied with ligands that react to the cell's EGFR, the cantilever is pushed and separated from the cell's surface to evaluate its binding forces.

Figure 7 shows the prototyped cantilever and the experimental setup. With a gold pad formed at the cantilever's tip, ligands are attached firmly onto it. Avidin-biotin binding is used to achieve this. First, taking advantage of the thiol's nature to form a self-assembled monolayer film on gold, carboxyl-containing thiol is applied to the gold film. Next, thiol-contained carboxyl avidin is prepared and biotin ligands are added to it, when selective binding occurs.

Figure 8 shows the receptors' binding forces which we

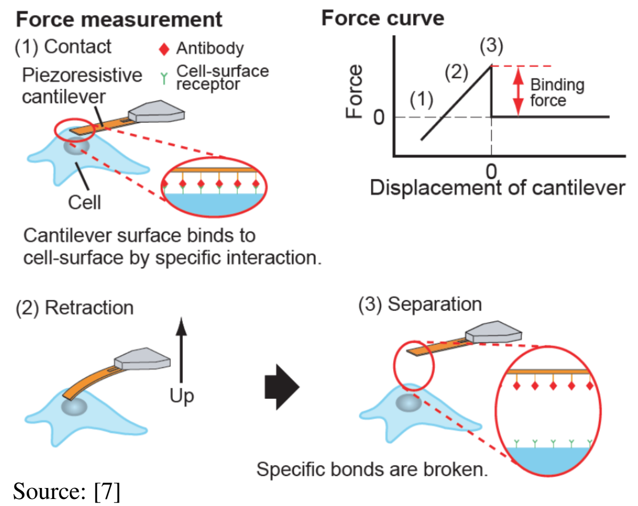

Source: [7]

Fig. 6. Measurement of receptors on cell surfaces [7].

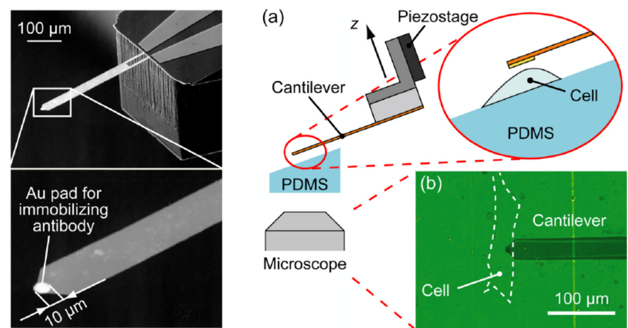

Fig. 7. Prototype piezo-resistive cantilever and experimental setup.

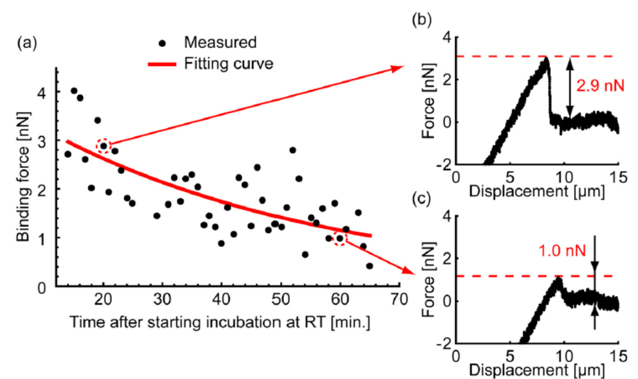

Source: [7]

Fig. 8. Changes in binding forces of receptors with time [7].

have measured using cells that are incubated at room temperature: the binding forces are measured with resolutions of 1 nN or less. While the binding force is 2.9 nN 20 minutes after the commencement of incubation, it decreases to 1.1 nN 60 minutes after the commencement of incubation. The decrease in the binding force signifies a decrease in the binding number of the EGFR and its ligands. This also suggests that the expression level of the receptor on the cell surface decreases with incubation time at room temperature.

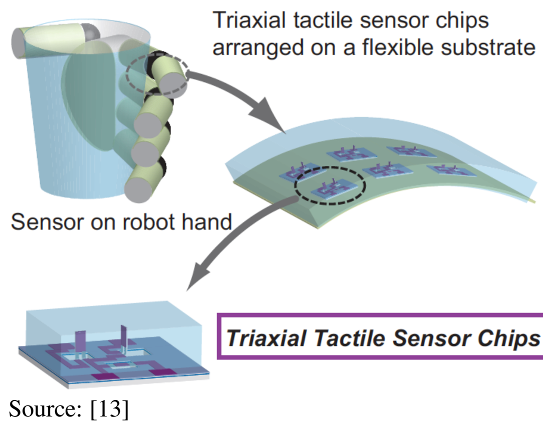

Source: [13]

Fig. 9. Tri-axial tactile sensor for robot hand [13].

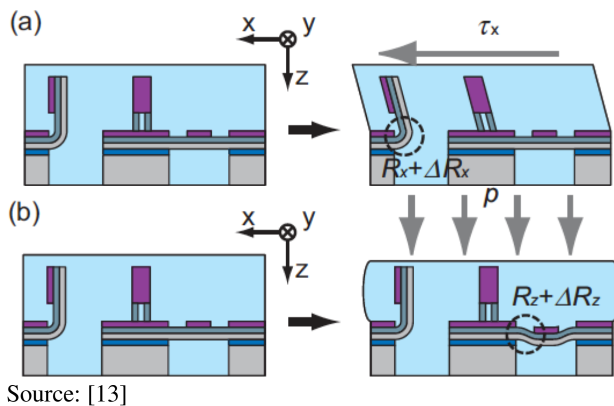

Source: [13]

Fig. 10. Tactile sensor's detection principle [13].

3.2. Devices Embedded into Elastic Body to Measure its Deformations

As piezo-resistive cantilevers embedded into an elastic body follow the body's deformations, the deformations can be detected as electric signals. The typical application for this phenomenon is tactile sensors, which include tri-axial tactile sensors [11], flexible sensors to be arranged on a curved surface [12], tri-axial tactile sensor chips [13], tri-axial tactile sensors simulating the structure of skin [14, 15], and tactile sensors with differential characteristics [16].

Figure 9 shows a tri-axial tactile sensor placed on a robot hand [13], which consists of a detection chip with a piezo-resistive cantilever embedded into the silicon rubber (PDMS). With the detection chip unit installed on the robot hand, it can detect one-axial forces in the pressure direction when it grasps an object, as well as two-axial shearing stress in the orthogonal slip directions.

Figure 10 shows the tri-axial tactile sensor's detection principle: when the shearing stress τ_x acts in the x-axis direction, the elastic material gets deformed as shown in **Fig. 10(a)**, which is detected by the x-axis piezo-resistive cantilever, but the piezo-resistive cantilever in the orthogonal y-axis direction does not react to the deformations because the piezo-resistance changes at the two hinged parts of the piezo-resistive cantilever are mutually cancelled. **Fig. 10(b)** shows the structure to detect the stress

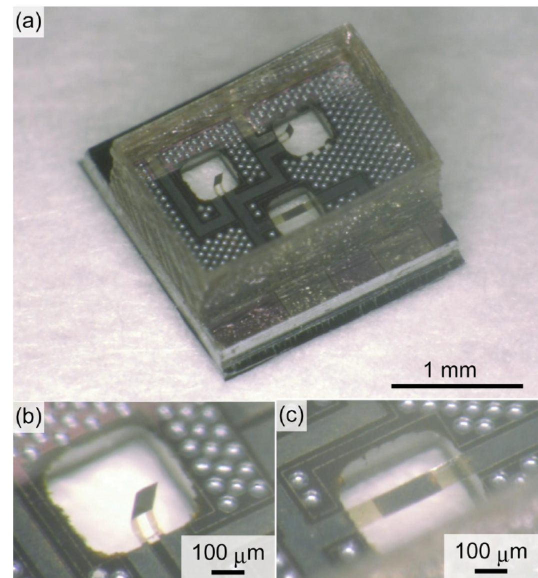

Source: [13]

Fig. 11. Prototyped tri-axial tactile sensor chip [13].

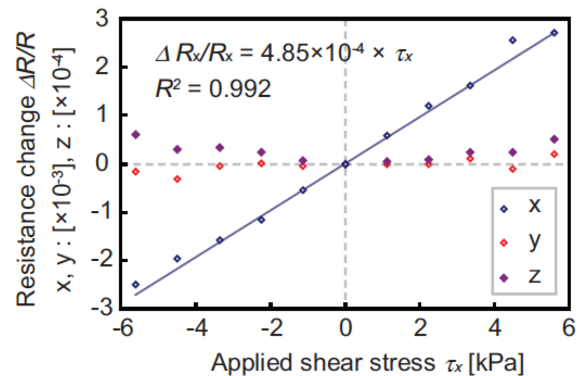

Fig. 12. Detection characteristics for shearing stress in x-axis direction.

in the z-axis direction, which is not a cantilever, but a double-supported beam with piezo-resistive parts at both ends of the beam.

Figure 11 shows the prototyped sensor chip, 2 mm^2 in size. **Fig. 11(b)** shows the piezo-resistive cantilever to detect shearing stress in the y-axis direction, which is 300 nm thick, 300 μm long, and 25 μm wide at the hinged part, and has a resistance value of about 2 kΩ. **Fig. 11(c)** shows the double-supported beam, which is 300 nm thick, 400 μm long, and 80 μm wide, and has a resistance value of about 0.5 kΩ.

Figure 12 shows the sensor chip's detection characteristics: the piezo-resistive cantilever to detect the shearing stress in the x-axis direction has a resistance change rate of 485 $\mu\varepsilon$/kPa on average, as well as a very good linearity; its sensitivity to z-directional stress is 395 $\mu\varepsilon$/kPa.

Figure 13 shows an array of prototyped sensor chips: 4 $\times$ 4 chips are embedded into 3-mm-thick PDMS. The sensor chips can be arranged on a curved surface, as shown in **Fig. 13**.

Presented below is an application example of tactile

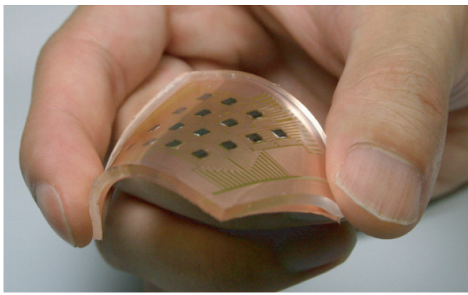

Source: [13]

Fig. 13. Prototyped tri-axial tactile sensor array [13].

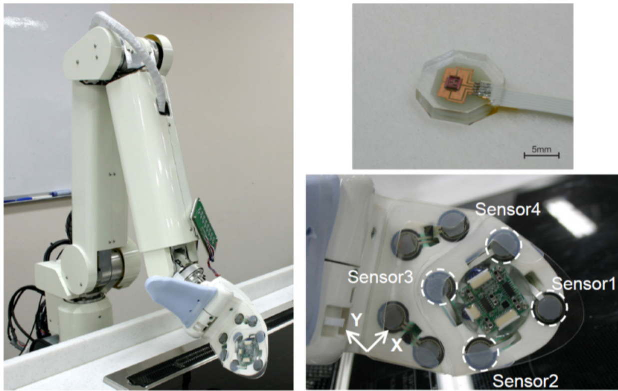

Fig. 14. Tri-axial tactile sensors installed on robot hand.

sensors: a housework support robot to support the aging society with fewer children [17]. **Fig. 14** shows tri-axial tactile sensors placed on the hand of a kitchen robot to handle dishes. It can determine the slipperiness of the dishes from the tactile information, and handle the dishes and cups with appropriate gripping forces.

3.3. Devices to Measure Airflow and Vibrations

Piezo-resistive cantilevers can be used to measure airflow rates, as well as sounds deriving from dynamic airflow changes. Previous studies include a study to measure the airflow at the leading edge of an ornithopter's wing [18], a study to evaluate the airflow resistance of thrips' wings [19], and a study on particle sensors [20]. Previous studies to measure sounds include ultrasonic sensors using air column resonance [21], ultrasonic sensors using Helmholtz resonance [22], and a study to search for sound sources using a resonance tube [23].

Presented below is a particle sensor using a piezo-resistive cantilever [20]. As a particle sensor to measure the cleanliness of air in clean rooms uses the principle of detecting light scattered from light-irradiated particles, it needs a laser diode to emit light, a photo diode to measure the scattered light, and a lens system to concentrate the laser beam and scattered light. Therefore, we have used cantilevers to construct a more simply structured particle sensor.

Figure 15 shows the construction of a particle sensor. Airflow is generated and a cantilever is arranged within it. The airflow can be measured from the lowfrequency

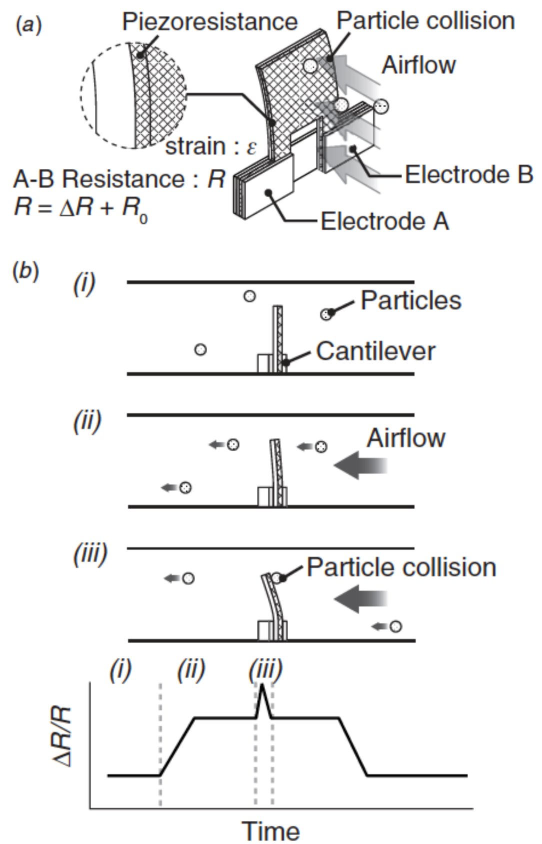

Source: [20]

Fig. 15. Particle sensor using piezo-resistive cantilever [20].

components of the cantilever's output. As vibrations are generated when particles collide with the cantilever, the number of particles that collide with the cantilever can be measured from the number of generated vibrations; then, the number of particles per unit volume of air can be calculated from the airflow and the number of collided particles.

Figure 16(a) shows particles colliding with the cantilever: (i) to (v) are photos of collisions at $t = 0.8$, 0.9, 1.0, 1.1 and 1.2 ms, respectively; particles collide at $t =$ 0.9 ms and then are dispersed. **Fig. 16(b)** shows the cantilever's output waveforms when particles collide with it. The collisions of particles excite the cantilever's vibrations, making the cantilever vibrate with its natural frequency. **Fig. 16(c)** shows the relationship between airflow velocity and the cantilever's output amplitude when particles collide with it. As particles of same size are used in the experiments, the airflow velocity and output amplitude are correlated with each other.

Reference [21] reports a study on ultrasonic sensors combining piezo-resistive cantilevers with the air-column resonance phenomenon caused by the cavities. Those ultrasonic sensors, where the cavities resonate with and amplify specific frequencies of ultrasonic waves only, have such sharp frequency characteristics that they should be less susceptible to attenuation or disturbances.

Figure 17 shows the structure of the above-mentioned ultrasonic sensor; cavities that can make air-column reso-

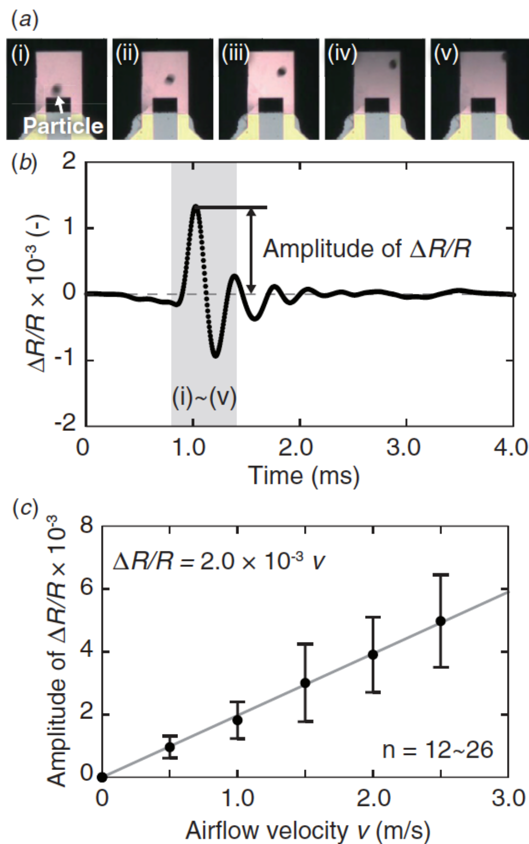

Source: [20]

Fig. 16. Collision of particles and sensor's output [20].

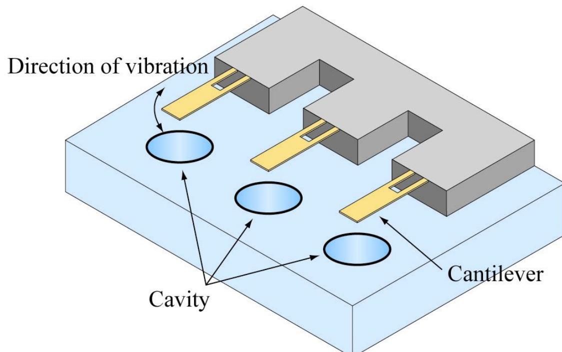

Source: [21]

Fig. 17. Ultrasonic sensor using air-column resonance [21].

nances of 1/4 wave length are arranged below the piezo-resistive cantilevers. **Fig. 18** shows the prototyped ultrasonic sensor. The cantilever is 300 nm thick, 16 μm wide, and 80 μ m long. The cantilever and the cavity are both designed to have a resonance frequency of 30 kHz.

Figure 19 shows the evaluation results of the ultrasonic sensor's output in response to ultrasonic waves. A single cantilever has a resonance frequency of 30.7 kHz, and the sensor's output voltage in response to ultrasonic waves of constant output from a distance of 50 mm is 38.4 mV; with a cavity arranged below the cantilever, the sensor's output voltage reaches a maximum of 475 mV in response to a resonance frequency of 30.9 kHz. This demonstrates that

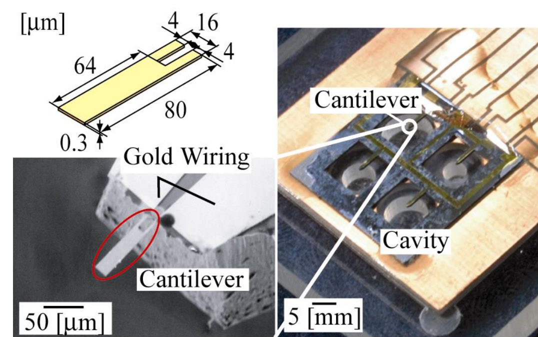

Fig. 18. Prototyped ultrasonic sensors.

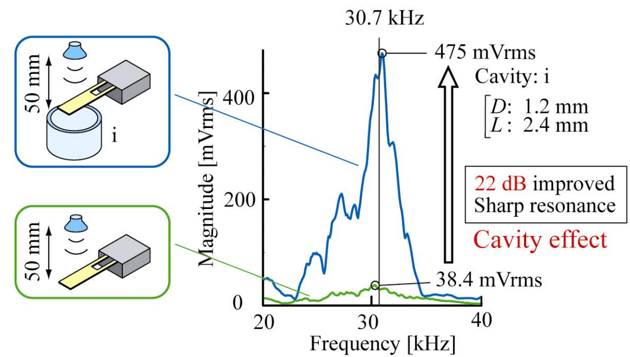

Fig. 19. Air-column resonance effects.

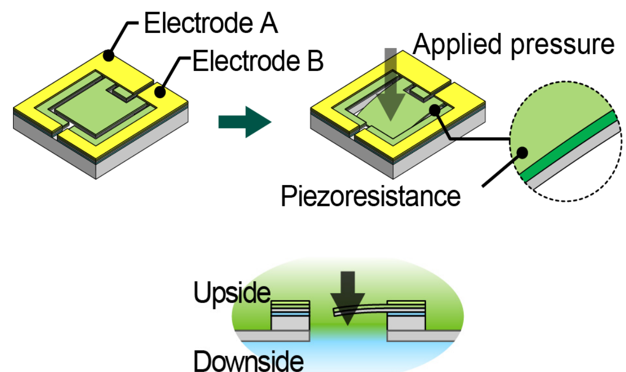

Fig. 20. Differential pressure sensor's structure and its operation.

the sensitivity has improved by 22 dB due to the cavity effects. We can also see from **Fig. 19** that the sensor's resonance characteristics have become sharper.

3.4. Devices to Measure Differential Air Pressure

The differential pressure between the upside and downside of the piezo-resistive cantilever can be measured by narrowing the gap between the cantilever and its surroundings to make it more difficult for air to pass through. **Fig. 20** shows the structure of a differential pressure sensor and its operation. The cantilever shown in **Fig. 1** has exactly the same structure: the size of the cantilever's pressure-receiving side is 100 μm $\times$ 100 μm, whereas the gap between the cantilever and its surroundings is 5 μm [3]. Its sensitivity to detect differential pressure is as high as to deliver resolutions of 0.02 Pa. Presented below

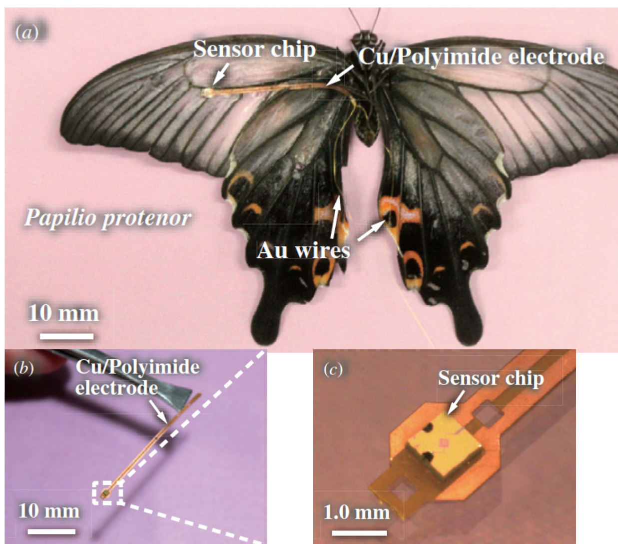

(b) Cu/Polyimide electrode 10 mm (c) Sensor chip 1.0 mm

Source: [28]

Fig. 21. Differential pressure sensor placed on butterfly's wings [28].

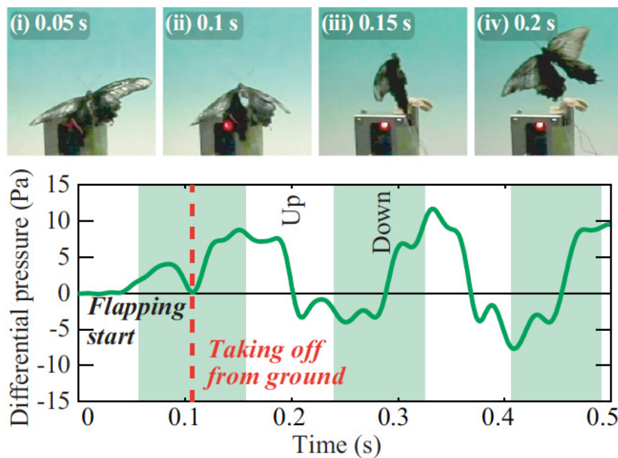

Source: [27]

Fig. 22. Changes in wing pressure of a flying butterfly [27].

are some of the studies to measure the surface pressure of wings using differential pressure sensors, which include a study to measure the surface pressure of artificial wings [24], studies to measure pressure on the wings of a flying ornithopter [25, 26], and studies to measure surface pressure of a butterfly's wings [27, 28]. Also available is a study to construct a three-dimensional wind-velocity sensor using a differential pressure sensor [29].

Presented below is an example of measuring the pressure on the wings of a flying butterfly with a differential pressure sensor placed on its wings [28]. **Fig. 21** shows a differential pressure sensor placed on the wings of a butterfly. As the gross weight of the sensor chip and wiring is 4.5 mg, 10% or less than that of the butterfly's wing, they are not expected to adversely affect the butterfly's flying.

Figure 22 shows the changes in the wing pressure of a flying butterfly [27]. The detailed measurements [28] show the average absolute values of the measured pres-

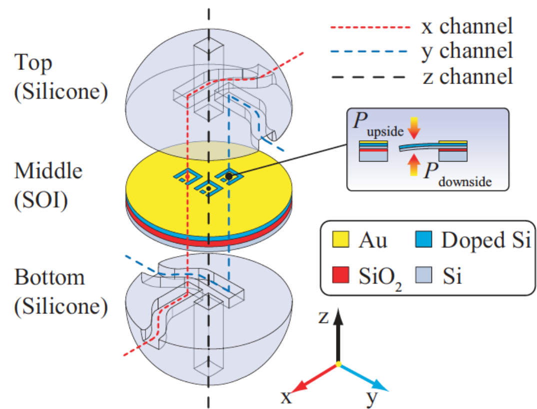

Source: [29]

Fig. 23. Structure of a three-dimensional wind-velocity sensor [29].

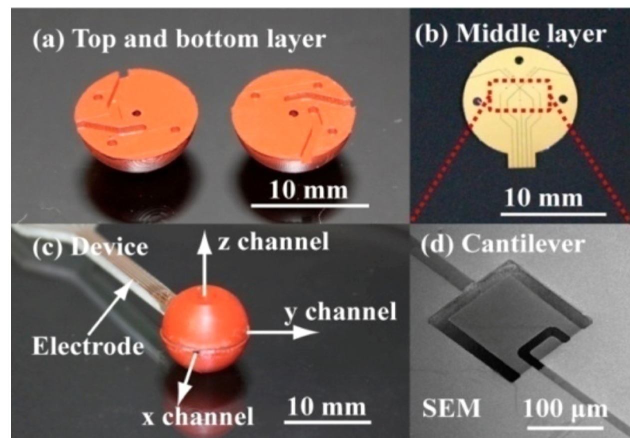

Fig. 24. Prototyped three-dimensional wind-velocity sensor.

sure; 7.4, 5.5, and 2.1 Pa at the tip, middle, and base of the front wing, respectively, and 2.1 Pa at the middle of the rear wing. A momentary value of pressure acting on the front wing amounts to 10 Pa, ten times greater than the butterfly's wing surface load.

Hot-wire anemometers to measure the heat radiated from a heated object are mainly used as sensors to measure wind velocities, but can not measure wind direction three-dimensionally. Sensors that can measure wind velocities three-dimensionally are developed by combining a cantilever-fitted differential-pressure sensor and flow channels [29].

Figure 23 shows the structure of a three-dimensional wind-velocity sensor: there are three differential-pressure sensors arranged in the SOI substrate surface; the substrate is sandwiched on both upside and downside by silicon-rubber structures with channels extended in the *x*-, *y*- and *z*-directions. **Fig. 24** shows a photo of the prototyped wind-velocity sensor: its external form is ball-shaped with a 10 mm diameter.

Figure 25 shows the results of the wind-velocity measuring experiments. With wind flowing through the wind tunnel, the sensor is rotated around the *y*-axis, orthogonal to the wind flow, and the output of each axis is plotted.

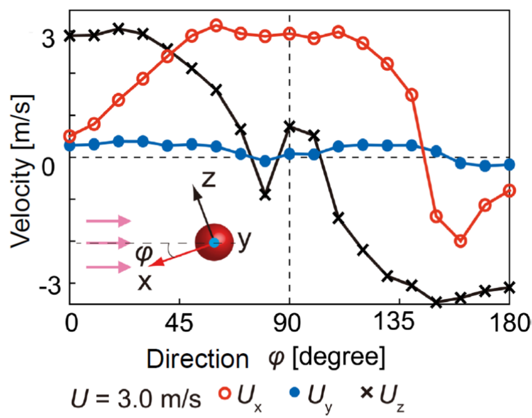

Fig. 25. Example of wind-velocity detection characteristics.

These plots are generally sine- and cosine-types, as expected; the irregular plots of the z-axis output near 90° seem attributable to the printed circuit board to draw out the wiring. The error in the measurement of 3 m/s wind is about 0.4 m/s (RMSE).

3.5. Devices to Measure Differential Pressure Between Cavities and External Environment

The external pressure, with reference to the pressure on the cavities, can be measured by arranging the cavities below the piezo-resistive cantilevers. Previous studies applying the above-mentioned method include studies on high-sensitivity air-pressure sensors [30, 31], a study on absolute pressure sensors with the cantilever gap sealed with liquid [32], and a study on underwater microphones [33].

It is difficult to enhance the sensitivity of general air-pressure sensors because they use diaphragms and sealed-type cavities. In References [30] and [31] air-pressure sensors using cantilevers and unsealed cavities are proposed in order to achieve high-sensitivity sensors. **Fig. 26** shows the structure of the proposed air-pressure sensor: there are cavities arranged below the cantilevers using differential pressure sensors. The air gap between the cantilever and the surroundings is 1.7 μm. Any difference in air pressure between the cavity's inside and outside will generate airflow into and out of the cavities, and such airflows are measured with the cantilevers. Once the airflows are generated, any difference in air pressure between the cavity's inside and outside is eliminated, and the sensor's output becomes zero. In other words, the proposed air-pressure sensor outputs changes in air pressure, or values proportional to the derivatives of such air-pressure changes.

Figure 27 shows the waveforms detected when the air-pressure sensor is walked down the eleven-step stairs: the amplitude of the waveforms is about 1500 $\mu\varepsilon_{\mathrm{p-p}}$. **Fig. 27 (bottom)** shows the integrated waveforms, from which we can see that the eleven stair steps, each 18 cm high, are accurately reproduced.

Figure 28 shows the sensor enabled to detect absolute air pressure by sealing the cantilever's gap with liquid to

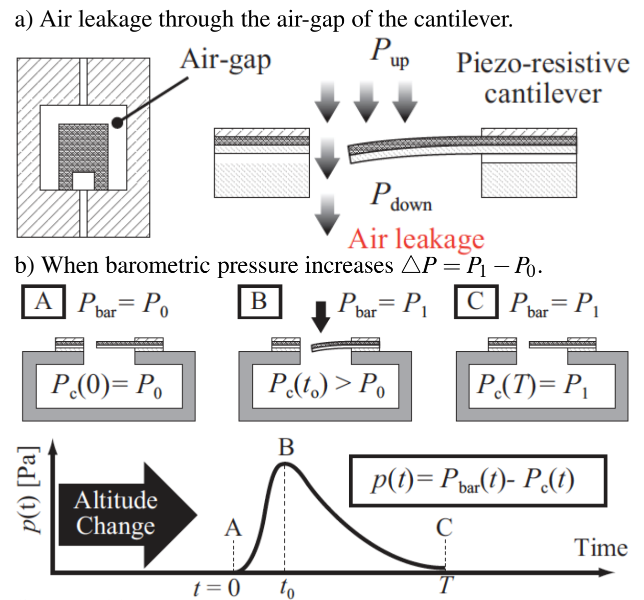

Fig. 26. Air-pressure detecting sensor with cantilevers and cavities [30].

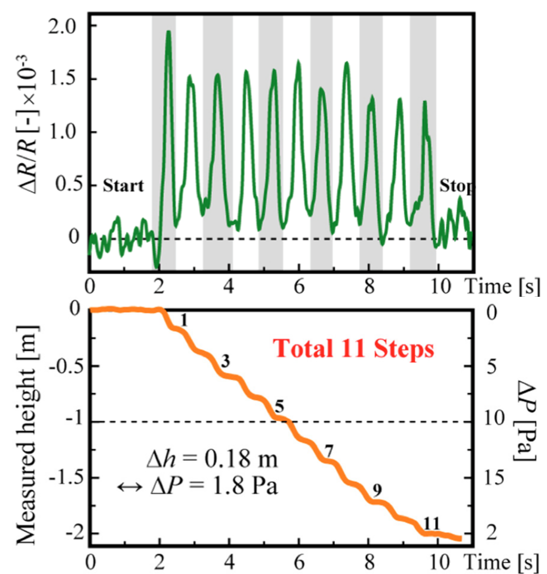

Fig. 27. Waveforms detected with sensor walking down stairs.

prevent air from flowing into and out of the gap [32]. This sensor, placed in water, can work as an underwater microphone [33].

3.6. Devices with Cantilevers Arranged on a Liquid Interface

Device with piezo-cantilevers arranged on an interface between liquid and air, where the cantilever's motion follows that of the liquid interface, can detect waves on the liquid interface or on the liquid surface. As a cantilever's sensitivity to frequencies higher than its natural frequency decreases in air, it cannot extend its detectable frequency band very far. However, a device with piezo-resistive cantilevers arranged on a liquid interface, where the can-

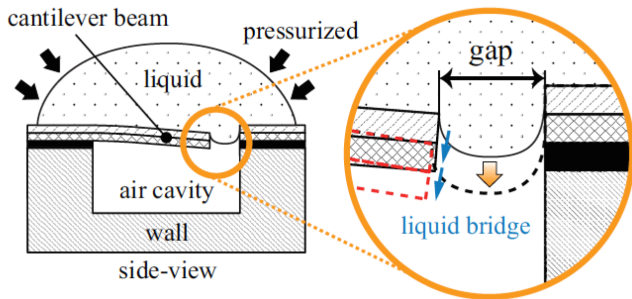

Fig. 28. Absolute air-pressure detecting sensor.

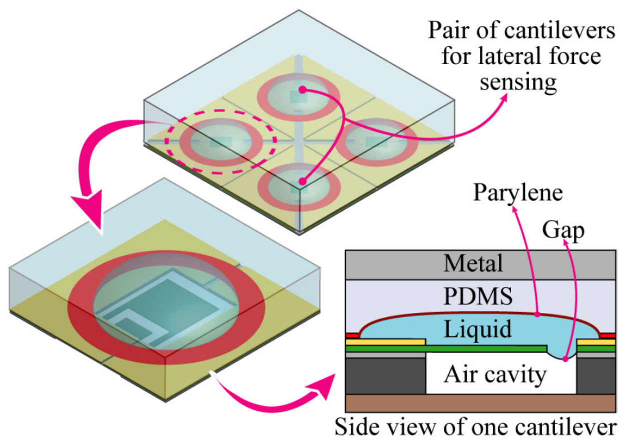

Source: [36]

Fig. 29. Structure of wide-band force sensor [36].

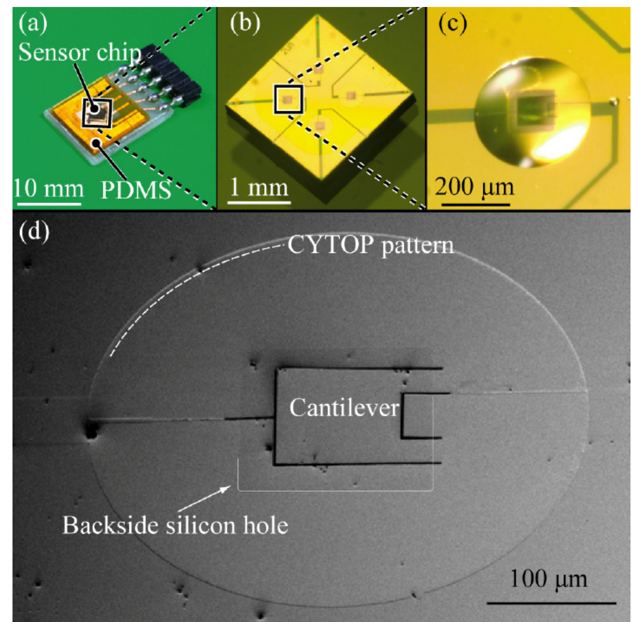

Source: [36]

Fig. 30. Photo of prototyped wide-band force sensor [36].

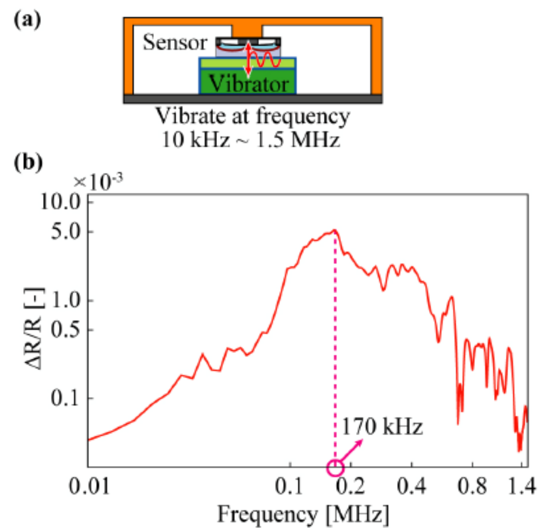

Source: [36]

Fig. 31. Frequency characteristics of wide-band force sensor [36].

tilevers are deformed following the waves on the liquid surface, can extend its detectable frequency band to frequencies much higher than its natural frequency in air. As the latter device detects vibrations via liquid, it can easily interface with any objects to be measured.

Previous studies on measurements using the above-mentioned principle include measurements of muscle sounds [34] and a study on pulse wave propagation [35]. Previous studies using the above-mentioned wide-band detection characteristics include a study on wide-band force sensors [36] and wide-band musclesound sensors [37]. Current studies using the wide-band characteristics of device with double-supported beams instead of cantilevers arranged on the interface include: a study on acoustic emission (AE) sensors [38] and a study on measurements of elastic waves with AE sensors [39].

Figure 29 shows the structure of the wide-band force sensor [36]. A liquid is placed on the piezo-resistive cantilever, and the liquid is sealed by directly vapor-depositing Parylene on it. Forces and vibrations are propagated to the cantilever via the multi-layer structure. The four detection units are to detect not only forces in the pressure direction, but also those in the shearing direction by taking the differences between the detection units. Despite a gap of 2 μm between the cantilever's surroundings and the side wall, the liquid never leaks through the gap. **Fig. 30** shows a photo of the prototyped sensor. The load testing proves that the sensor has a high linearity in the range of 40 kPa in the pressure direction and 30 kPa in the shearing direction. **Fig. 31** shows the response characteristics of the wide-band sensor when it is vibrated in the pressure direction. We can see from **Fig. 31** that with a resonance peak appearing at 170 kHz, the sensor can detect frequencies up to 1 MHz or more.

The study on AE sensors [38] makes use of the wide-band force sensor's capability of detecting higher frequencies. When cracks progress in concrete or steel materials, ultrasonic vibrations, called acoustic emissions, occur. Such ultrasonic vibrations have a peak at 50 kHz in concrete and at 200 kHz in steel materials. **Fig. 32** shows the AE sensor's structure. Although its detection part is located on the liquid interface, in the same manner as other types of force sensors, it uses a double-supported

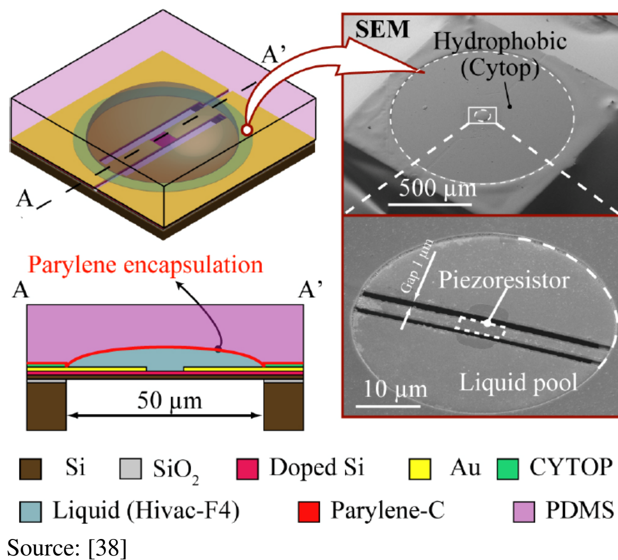

Fig. 32. Structure of acoustic emission (AE) sensor [38].

beam instead of a cantilever to ensure that in no event should the liquid leak. A study to monitor infrastructures with AE sensors is now underway [39].

4. Conclusions

We have proposed a large number of sensor devices that use piezo-resistive cantilevers. The proposed sensor devices have force resolutions of around 10 pN by using cantilevers as thin as 300 nm. Applying the above-mentioned piezo-resistive cantilevers, we have engaged in researching and developing the following devices and sensors: a device to measure object-contacting forces, a tactile sensor embedded into an elastic body, a particle sensor to measure air flow, an ultrasonic microphone, a differential pressure sensor to measure the pressure acting on wings, a sensor to measure differential pressure between cavities and external environment, and a wide-band sensor with cantilevers arranged on a liquid interface. We hope that piezo-resistive cantilevers will find increasingly wider applications in future.

References:

[1] M. Tortonese, R. C. Barrett, and C. F. Quate, "Atomic resolution with an atomic force microscope using piezoresistive detection," Applied Physics Letters, Vol.62, No.8, pp. 834-836, 1993.

[2] M. Gel and I. Shimoyama, "Force sensing submicrometer thick cantilevers with ultra-thin piezoresistors by rapid thermal diffusion," J. of Micromechanics and Microengineering, Vol.14, No.3, pp. 423-428, 2003.

[3] H. Takahashi, N. Minh Dung, K. Matsumoto, and I. Shimoyama, "Differential pressure sensor using a piezoresistive cantilever," J. of Micromechanics and Microengineering, Vol.22, No.5, Article Number 055015, 2012.

[4] H. Onoe, M. Gel, K. Hoshino, K. Matsumoto, and I. Shimoyama, "Direct measurement of the binding force between micro-fabricated particles and a planar surface in aqueous solution by force-sensing piezoresistive cantilevers," Langmuir, Vol.21, No.24, pp. 11251-11261, 2005.

[5] T. Kan, K. Matsumoto, and I. Shimoyama, "Piezoresistor-equipped fluorescence-based cantilever probe for near-field scanning," Review of Scientific Instruments, Vol.78, No.8, Article Number 083106, 2007.

[6] K. Kuwana, K. Matsumoto, and I. Shimoyama, "Measurementa of Binding Force between a Receptor-coated Cantilever and a Ligand-coated Surface for Protein Sensor," The 11th Int. Conf. on Miniaturized Systems for Chemistry and Life Sciences (uTAS2007), pp. 1095-1097, 2007.

[7] K. Kuwana, Y. J. Heo, K. Matsumoto, and I. Shimoyama, "Measurement Method of Cell-surface Receptor Concentration Using Antibody Conjugated Piezoresistive Cantilever," The 13th Int. Conf. on Miniaturized Systems for Chemistry and Life Sciences(microTAS2009), pp. 2022-2024, 2009.

[8] T. V. Nguyen, M. D. Nguyen, H. Takahashi, K. Matsumoto, and I. Shimoyama, "Viscosity measurement based on the tapping-induced free vibration of sessile droplets using MEMS-based piezoresistive cantilevers," Lab on a Chip, The Royal Society of Chemistry, Vol.15, No.18, pp. 3670-3676, 2015.

[9] T. V. Nguyen , K. Matsumoto, and I. Shimoyama, "A Viscometer Based on Vibration of Droplets on a Piezoresistive Cantilever Array," The 28th IEEE Int. Conf. on Micro Electro Mechanical Systems (MEMS '15), 2015.

[10] T. V. Nguyen, K. Matsumoto, and I. Shimoyama, "Pressure Distribution on the Contact Area During the Impact of a Droplet on a Textured Surface," The 29th IEEE Int. Conf. on Micro Electro Mechanical Systems (MEMS '16), 2016.

[11] K. Noda, K. Hoshino, K. Matsumoto, and I. Shimoyama, " A Shear Stress Sensor for Tactile Sensing with the Piezoresistive Cantilever Standing in Elastic Material," Sensors and Actuators A: Physical, Vol.127, No.2, pp. 295-301, 2006.

[12] K. Noda, H. Onoe, E. Iwase, K. Matsumoto, and I. Shimoyama, "Flexible tactile sensor for shear stress measurement using transferred sub-μ m-thick Si piezoresistive cantilevers," J. of Micromechanics and Microengineering, Vol.22, No.11, article No.115025, 2012.

[13] Y. Tanaka, A. Nakai, E. Iwase, T. Goto, K. Matsumoto, and I. Shimoyama, "Triaxial Tactile Sensor Chips with Piezoresistive Cantilevers Mountable on Curved Surface," Asia-Pacific Conf. on Transducers and Micro-Nano Technology 2008 (APCOT2008), pp. 1B1-1, 2008.

[14] K. Noda, K. Matsumoto, and I. Shimoyama, "Tactile sensor with standing piezoresistive cantilevers covered with 2-layer skin type structures for texture detection of object surface," The 2008 IEEE/RSJ Int. Conf. on Intelligent Robots and Systems (IROS2008), pp. 3953-3958, 2008.

[15] K. Noda, K. Matsumoto, and I. Shimoyama, "Skin-type Tactile Sensor Using Standing Piezoresistive Cantilever for Micro Structure Detection," The 9th Annual IEEE Conf. on Sensors (Sensors2010), pp. 2089-2092, 2010.

[16] K. Noda, K. Matsumoto, and I. Shimoyama, "Flexible tactile sensor sheet with liquid filter for shear force detection," The 22nd IEEE Int. Conf. on Micro Electro Mechanical Systems (MEMS '09), pp. 785-788, 2009.

[17] K. Yamazaki, R. Ueda, S. Nozawa, M. Kojima, K. Okada, K. Matsumoto, M. Ishikawa, I. Shimoyama, and M. Inaba, "Home-Assistant Robot for an Aging Society," Procs. of the IEEE, Vol.100, No.8, pp. 2429-2441, 2012.

[18] H. Takahashi, E. Iwase, K. Matsumoto, and I. Shimoyama, "Air Flow Senser for an Insect-Like Flapping Wing," The 21st IEEE Int. Conf. on Micro Electro Mechanical Systems (MEMS '08), pp. 916-919, 2008.

[19] H. Takahashi, K. Sato, M. D. Nguyen, K. Matsumoto, and I. Shimoyama, "Characteristic evaluation of a bristled wing using mechanical models of a thrips wings with MEMS piezoresistive cantilevers," J. of Biomechanical Science and Engineering, Vol.10, No.2, paper No.14-00233, 2014.

[20] H. Takahashi, T. Kan, K. Matsumoto, and I. Shimoyama, "Simultaneous detection of particles and airflow with a MEMS piezoresistive cantilever," Measurement Science and Technology, Vol.24, No.2, article No.025107, 2013.

[21] S. Yoshimi, K. Hoshino, K. Matsumoto, and I. Shimoyama, "A Cantilever Microphone Using Resonance of Closed-End Air Columns," The 19th Int. Conf. on Micro Electro Mechanical Systems (MEMS '06), pp. 574-577, 2006.

[22] H. Takahashi, A. Suzuki, E. Iwase, K. Matsumoto, and I. Shimoyama, "MEMS microphone with a micro Helmholtz resonator," J. of Micromechanics and Microengineering, Vol.22, No.8, article No.085019, 2012.

[23] M. D. Nguyen, A. Inaba, H. Takahashi, E. Iwase, K. Matsumoto, and I. Shimoyama, "Sound Direction Sensor with an Acoustic Channel," Procs. of the 23rd IEEE Int. Conf. on Micro Electro Mechanical Systems (MEMS2010), pp. 655-658, 2010.

[24] H. Takahashi, K. Matsumoto, and I. Shimoyama, "Air pressure sensor for an insect wing," The 22nd IEEE Int. Conf. on Micro Electro Mechanical Systems (MEMS '09), pp. 825-828, 2009.
[25] H. Takahashi, Y. Aoyama, K. Ohsawa, H. Tanaka, E. Iwase, K. Matsumoto, and I. Shimoyama, "Differential Pressure Measurement Using A Free-Flying Insect-Like Ornithopter with A MEMS Sensor," Bioinspiration and Biomimetics, Vol.5, No.3, 036005, 2010.
[26] H. Takahashi, K. Sato, K. Matsumoto, and I. Shimoyama, "Measuring differential pressures with multiple MEMS sensors during takeoff of an insect-like ornithopter," J. of Biomechanical Science and Engineering, Vol.9, No.1, article No.JBSE0004, 2014.
[27] H. Takahashi, K. Matsumoto, and I. Shimoyama, "Measurement of Differential Pressure on a Butterfly Wing," Procs. of the 23rd IEEE Int. Conf. on Micro Electro Mechanical Systems (MEMS2010), pp. 63-66, 2010.
[28] H. Takahashi, H. Tanaka, K. Matsumoto, and I. Shimoyama, "Differential pressure distribution measurement with an MEMS sensor on a free-flying butterfly wing," Bioinspiration & Biomimetics, Vol.7, No.036020, 2012.
[29] M. D. Nguyen, H. Takahashi, K. Kuwana, T. Takahata, K. Matsumoto, and I. Shimoyama, "3D Airflow Velocity Vector Sensor," The 24th IEEE Int. Conf. on Micro Electro Mechanical Systems (MEMS '11), pp. 513-516, 2011.
[30] M. D. Nguyen, H. Takahashi, K. Matsumoto, and I. Shimoyama, "Barometric pressure change measurement," The 16th Int. Conf. on Solid-State Sensors, Actuators and Microsystems (Transducers2011), pp. 898-901, 2011.
[31] M. D. Nguyen, H. Takahashi, T. Uchiyama, K. Matsumoto, and I. Shimoyama, "A barometric pressure sensor based on the air-gap scale effect in a cantilever," Applied Physics Letters, Vol.103, No.14, article No.143505, 2013.
[32] M. D. Nguyen, H. P. Phan, K. Matsumoto, and I. Shimoyama, "A Sensitive Liquid-Cantilever Diaphragm for Pressure Sensor," The 26th IEEE Int. Conf. on Micro Electro Mechanical Systems (MEMS '13), 2013.
[33] M. D. Nguyen, H. P. Phan, K. Matsumoto, and I. Shimoyama, "A Hydrophone Using Liquid to Bridge the Gap of a Piezo-Resistive Cantilever," The 17th Int. Conf. on Solid-State Sensors, Actuators and Microsystems (Transducers), 2013.
[34] T. Kaneko, M. D. Nguyen, R. Aoki, T. Takahata, K. Matsumoto, and I. Shimoyama, "Measurement of Mechanomyogram," The 27th IEEE Int. Conf. on Micro Electro Mechanical Systems (MEMS '14), 2014.
[35] T. Kaneko, M. D. Nguyen, Q. K. Pham, Y. Takei, T. Takahata, K. Matsumoto, and I. Shimoyama, "Pulse Wave Measurement in Human Using Piezoresistive Cantilever on Liquid," The 28th IEEE Int. Conf. on Micro Electro Mechanical Systems (MEMS '15), 2015.
[36] Q. K. Pham, M. D. Nguyen, B. K. Nguyen, H. P. Phan, K. Matsumoto, and I. Shimoyama, "Multi-Axis Force Sensor with Dynamic Range up to Ultrasonic," The 27th IEEE Int. Conf. on Micro Electro Mechanical Systems (MEMS '14), 2014.
[37] R. Aoki, Y. Takei, M. D. Nguyen, T. Takahata, K. Matsumoto, and I. Shimoyama, "Detection of High-Frequency Component of Mechanomyogram," The 29th IEEE Int. Conf. on Micro Electro Mechanical Systems (MEMS '16), 2016.
[38] Q. K. Pham, M. D. Nguyen, K. Matsumoto, and I. Shimoyama, "Acoustic Emission Sensor Using Liquid-On-Beam Structure," The 18th Int. Conf. on Solid-State Sensors, Actuators and Microsystems (Transducers), 2015.
[39] T. Omori, T. Usui, K. Watabe, M. D. Nguyen, K. Matsumoto, and I. Shimoyama, "Elastic wave measurement using a MEMS AE sensor," 8th Int. Conf. on Acoustic Emission, Kyoto, Japan, December 5-9, pp. 339-344, 2016.

Name:
Kiyoshi Matsumoto

Affiliation:
Professor, Department of Mechanical Engineering, Faculty of Science and Engineering, Toyo University

Address:
2100 Kujirai, Kawagoe, Saitama 350-8585, Japan

Brief Biographical History:
2000- Associate Professor, The University of Tokyo
2006- Project Professor, The University of Tokyo
2016- Professor, Toyo University

Main Works:
- Robotics, Sensors and Microsystems

Membership in Academic Societies:
- Japan Society of Mechanical Engineers (JSME)
- Robotics Society of Japan (RSJ)

Name:
Isao Shimoyama

Affiliation:
Professor, Department of Mechano-Informatics, Graduate School of Information Science and Technology, The University of Tokyo

Address:
7-3-1 Hongo, Bunkyo, Tokyo 113-8656, Japan

Brief Biographical History:
1982- Lecturer, The University of Tokyo
1983- Associate Professor, The University of Tokyo
1998- Professor, The University of Tokyo

Main Works:
- Robotics and MEMS (Micro-Electro-Mechanical Systems)

Membership in Academic Societies:
- Japan Society of Mechanical Engineers (JSME)
- Robotics Society of Japan (RSJ)